6A.2 MISOVORTICES AND BOUNDARIES WITHIN THE 7 JANUARY 2014 LONG LAKE-AXIS-PARALLEL (LLAP) LAKE-EFFECT SNOW BAND DURING THE ONTARIO WINTER LAKE-EFFECT SYSTEMS (OWLeS) PROJECT

Jake P. Mulholland*, Jeffrey W. Frame
University of Illinois at Urbana-Champaign, Urbana, Illinois

Scott M. Steiger
State University of New York at Oswego, Oswego, New York

1. INTRODUCTION

The winter of 2013-2014 featured an extensive field campaign to study lake-effect snow storms called the Ontario Winter Lake-effect Systems (OWLeS) Project. There were three main objectives of the project: 1) to examine the kinematics and dynamics of long lake-axis-parallel (LLAP; e.g., Steiger et al. 2013) snow bands, 2) upwind and downwind lake influences (i.e., heat and moisture fluxes/advection) on lake-effect convection, and 3) orographic influences on lake-effect convection. The platforms that were utilized during the project included: three X-band Doppler-on-Wheels (DOW) radars (provided by the Center for Severe Weather Research), five (four mobile) rawinsonde systems, the University of Wyoming King Air (UWKA) aircraft, and the University of Alabama at Huntsville's Mobile Integrated Profiling System (MIPS).

Previous lake-effect snow research has mainly focused on the western Great Lakes, such as Lake Michigan and Lake Superior. Studies such as Forbes and Merritt (1984) and Laird et al. (2001) documented instances of mesovortices (diameters [D] > 4000 m; Fujita 1981) forming over the lake during instances of weak background synoptic flow (e.g., Niziol et al. 1995, Type-V bands). The mesovortices typically appeared to either exhibit a braided structure or occur as a single vortex with an eye-like feature. These mesovortices were typically accompanied by weak cyclonic low-level rotation, brief bursts of heavier snow, and gusty winds (Forbes and Merritt 1984).

A more recent field campaign, the Long Lake-Axis-Parallel (LLAP) Project, occurred during the winter of 2010-2011 over Lake Ontario and surrounding downwind (i.e., south and east) locations. The main goal of this project was to obtain fine-scale Doppler radar observations of LLAP bands which had never been attempted before.

The project was a major success with some observations revealing the presence of mesovortices (D > 4000 m), misovortices (Fig. 1; D ~ 40-4000 m), horizontal vortices, horizontal shear zones (Fig. 1), bounded weak echo regions, outflow boundaries, and anvils (Steiger et al. 2013). The mesoscale vortices sometimes altered the morphology and orientation of the bands, which has implications for weather forecasters attempting to predict snowfall intensity, amount, and location. Hence, this research is aimed to understand the underlying dynamics of these miso- and mesovortices and the processes that aid in their development, maintenance, and ultimate demise. One event from the OWLeS project which demonstrated an abundance of misovortices was 7 January 2014. This case is the focus for this research.

2. OVERVIEW OF 7 JANUARY 2014 LAKE-EFFECT EVENT

Throughout the winter of 2013-2014, frequent intrusions of Arctic air masses occurred over most of the eastern 2/3^{rds} of the continental United States. 7 January 2014 was just one such case from this anomalously cold winter. The 0000 UTC/7 Jan 2014 Rapid Refresh (RAP) model 500-hPa analysis reveals a highly-amplified pattern with a deep trough over the eastern U.S. and a large ridge over the western U.S. (Fig. 2). A shortwave trough was located to the west of Lake Ontario, over northern Lower Michigan (Fig. 2). This shortwave trough traversed Lake Ontario between 0400-0800 UTC. Quasi-geostrophic forcing for ascent ahead of the approaching shortwave trough overspread the region, forcing the capping

* *Corresponding author address*: Jake P. Mulholland, University of Illinois at Urbana-Champaign, Dept. of Atmospheric Sciences, Urbana, IL, 61801; email: jmulhol2@illinois.edu

inversion atop the Arctic air mass over Lake Ontario to rise. A sounding launched from Henderson Harbor, NY, at 0816 UTC revealed a moist and conditionally unstable boundary layer extending vertically to around 540 hPa (Fig. 3). With 850-hPa temperatures around -25˚C above a lake with a surface water temperature around 3˚C, thermodynamic conditions were more than adequate for an intense LLAP band to develop, which was indeed the case as seen in Fig. 4.

One aspect of this case that is of particular interest for this research was the presence of misovortices and boundaries within the LLAP band. Fig. 5 displays a string of misovortices at 0524 UTC, with diameters (defined here as distance between local max/min values of radial velocity) ranging from 1-3 km and approximate regular spacing around 5 km. The misovortices were located along the northern edge of the band, corresponding to a sharp N-S horizontal gradient in reflectivity (Fig. 5a). Also, a cyclonic horizontal shear zone was present along which the misovortices were propagating, as seen by the faster inbound velocities (darker green colors) to the south of the misovortices and the slower inbound velocities (lighter green colors) seen to the north of the misovortices (Fig. 5b).

Fig. 6 at 0744 UTC reveals that the western edge of the string of misovortices was propagating from west-to-east across Lake Ontario. The shear zone was now closer to the center of the band, with the edges of the band appearing more diffuse in the reflectivity field. Further inspection of the background synoptic regime reveals that an upstream connection with another LLAP band over Georgian Bay was present from 0400-0800 UTC. This upstream connection ceased after 0800 UTC as low-level winds backed from northwesterly to westerly over Georgian Bay following the passage of the aforementioned 500-hPa shortwave trough and the approach of a 700-hPa ridge from the west (Fig 7). The downstream advection of heat and moisture from upstream lakes affecting downwind lake-effect storms has been well documented in the literature (e.g., Rodriguez et al. 2007). However, the misovortices in this case appear to display a dependence on Georgian Bay. Once the upstream connection ceased, the string of misovortices disappeared and instances of only isolated vortices prevailed throughout the remainder of the event.

A Weather Research and Forecasting (WRF) model simulation valid at 0700 UTC illustrates the string of vortices extending southeastward from Georgian Bay, where the vortices appear to originate, toward the eastern portions of Lake Ontario (Fig. 8). This simulation is consistent with observations from the King City, Ontario, radar that depict misovortices developing downwind of Georgian Bay and moving southeastward (not shown) toward Lake Ontario. It is worth noting that WSR-88D radar data within the band over the northwestern portions of Lake Ontario from Montague, NY (KTYX), and Buffalo, NY (KBUF), is sparse owing to the relatively shallow nature of the band (between 2-3 km deep) in comparison to the radar beam height in that area (i.e., the KBUF 0.5˚ beam height was approximately 2 km above ground level [AGL] at a distance of 120 km from the radar over NW Lake Ontario). This precludes any low-level (< 1 km AGL) radar observations of vortices or most other features of interest within the band in this region.

3. METHODOLOGY

Further inspection of the misovortices was made possible with the use of dual-Doppler (DD) analyses. Fig. 9 displays the asset map with the approximate DD lobe from DOW6 and DOW8 drawn in red. Using a two-pass Barnes analysis, data from these radars were mapped to a 40 x 40 km grid with a horizontal and vertical grid spacing of 250 m. The horizontal smoothing parameter used was 0.747 km^2 and the vertical smoothing parameter was 0.400 km^2.

4. DUAL-DOPPLER ANALYSES OF THE MISOVORTICES

Figs. 10-13 display a DD wind synthesis at 0524 UTC. A confluence zone is evident in Fig. 10 near the northern edge of the band near the 20 dBZ reflectivity contour. The confluence line is also aligned with the line of maximum updrafts at 500 m AGL. Maximum updraft speeds at this level are between 1.5 – 2.5 m s^{-1} (Fig. 11). The reasoning behind choosing 500 m AGL for analysis is that low-level vortex stretching is hypothesized to play a role in the strengthening of the misovortices, as most of the vortices are observed to weaken significantly above 1 km AGL.

The reflectivity appendages seen in Fig. 10 correspond to patches of enhanced positive vertical vorticity (roughly circular regions of purple shading) at 500 m AGL in Fig. 12 and likely arise from the advection of hydrometeors

around the northern sides of the circulations. The maximum value of vertical vorticity is on the order of 2.0 x 10^{-2} s^{-1}. This value is similar to the DD results from the International H_2O Project (IHOP_2002; Weckwerth et al. 2004), which examined misovortices forming along low-level convergence zones over the Southern Great Plains. The maximum vertical vorticity values derived from the DD analyses of the misovortices during IHOP were on the order of ~1.3 x 10^{-2} s^{-1} (Marquis et al. 2007).

Not surprisingly, this string of misovortices is along a horizontal wind shift near the northern edge of the band. Fig 13 illustrates higher values of the zonal wind component (~20 m s^{-1}) to the south of the confluence line (warm colors) while lower values of the zonal wind component (~5 m s^{-1}) are seen to the north of the confluence line (cool colors). This suggests that the misovortices were likely forming from horizontal shear instability (HSI). More on this hypothesis is found in section 5 below.

Figs. 14-17 display a DD wind synthesis at 0744 UTC. The confluence zone has shifted southward toward the center of the band and is more subtle (Fig. 14). The reflectivity structure associated with the band was also more symmetric at this time, whereas at 0524 UTC, the band was asymmetric with a sharp horizontal reflectivity gradient along the northern edge and a diffuse southern edge. The area covered by reflectivity values greater than 20 dBZ was also smaller by this time. Updraft speeds also decreased, with maximum values of ~2.5 m s^{-1} at 0524 UTC compared to ~2.0 m s^{-1} at 0744 UTC (Fig. 15). The ribbon of maximum updraft speeds was slightly north of the center of the band at this time.

Fig. 16 depicts the lack of a string of vortices at 0744 UTC as was seen in at 0524 UTC (Fig. 12). This transition is coincident with the passage of the 500-hPa shortwave trough and approach of the 700-hPa ridge and cessation of the upstream connection with Georgian Bay as discussed above. The maximum vertical vorticity values at 0744 UTC (Fig. 16) are only on the order of ~0.8 x 10^{-2} s^{-1} (as compared to ~2.0 x 10^{-2} s^{-1} at 0524 UTC). This reduction in vertical vorticity is a direct reflection of the decrease in meridional shear of the zonal wind, which is illustrated in Fig. 17, which likely removed the necessary condition for HSI. After this time, only isolated instances of misovortices were observed.

5. DISCUSSION & CONCLUSIONS

7 January 2014 featured a long-duration (> 20 h) LLAP band that affected regions downwind of Lake Ontario. This event also exhibited numerous instances of misovortices. A string of misovortices occurred between 0400-0800 UTC, followed by a regime consisting of only isolated misovortices. Georgian Bay appeared vital to the development of the string of misovortices because once the upstream connection ceased, the string of misovortices over Lake Ontario vanished. One hypothesis is that the geometry of Georgian Bay (Figs. 7 and 8), which forms a v-shape at its southeast end, favors a funneling effect of the low-level wind field, perhaps locally increasing convergence and favoring the spin-up of misovortices.

Another hypothesis for the development of the misovortices is horizontal shear instability (HSI). This has been hypothesized previously by Steiger et al. (2013). A conceptual model from Marquis et al. (2007) summarizes an ideal situation for misocyclogenesis during IHOP (see Fig. 14 from Marquis et al. 2007). More quantitative research needs to be conducted, including evaluating whether or not conditions necessary for HSI were present, to say more about this particular hypothesis.

A final unanswered question is more general: Why does the horizontal shear zone (along which the misovortices develop) form in the first place? This is the key question behind the misovortices associated with these LLAP bands. Could it be a result of the secondary circulation (i.e., in-up-out) within the LLAP band or is it more complicated (see Steiger et al. 2013, discussion section for some additional insight)? These are questions left for further inspection and future research. The continual push to understand the underlying mechanisms that govern the formation, maintenance, and demise of these convergence and shear zones, associated misovortices, and upstream connections will likely be particularly useful to operational forecasters concerned with snowfall amount, location, and intensity from these bands.

6. ACKNOWLEDGMENTS

The authors would like to thank the many participants of the OWLeS Project who collected data in often formidable and adverse weather conditions. We are also grateful to: Rachel Humphries and Paul Robinson of CSWR

who helped tremendously in the post-processing of the DOW data; Drs. Karen Kosiba and Joshua Wurman of CSWR for their insight into misovortices and their development and maintenance; Dr. Robert Ballentine, Dillon Ulrich, and Andrew Janiszeski of SUNY Oswego for assistance with the WRF simulation, Christopher Johnston of the University of Illinois at Urbana-Champaign for creating the asset map; David Wojtowicz of the University of Illinois at Urbana-Champaign for computing assistance; and Janice Mulholland for her useful comments on this paper. Support for this work was made possible by NSF Grant AGS 12-59257.

7. REFERENCES

Forbes, G. S., and J. H. Merritt, 1984: Mesoscale vortices over the Great Lakes in wintertime. *Mon. Wea. Rev.*, **112**, 377–381.

Fujita, T. T., 1981: Tornadoes and downbursts in the context of generalized planetary scales. *J. Atmos. Sci.*, **38**, 1511–1534.

Laird, N. F., L. J. Miller, and D. A. R. Kristovich, 2001: Synthetic dual-Doppler analysis of a winter mesoscale vortex. *Mon. Wea. Rev.*, **129**, 312–331.

Marquis, J. N., Y. P. Richardson, and J. M. Wurman, 2007: Kinematic observations of misocyclones along boundaries during IHOP. *Mon. Wea. Rev.*, **135**, 1749–1768.

Niziol, T. A., W. R. Snyder, and J. S. Waldstreicher, 1995: Winter weather forecasting throughout the eastern United States. Part IV: Lake effect snow. *Wea. Forecasting*, **10**, 61–77.

Rodriguez, Y., D. A. R. Kristovich, and M. R. Hjelmfelt, 2007: Lake-to-lake cloud bands: Frequencies and locations. *Mon. Wea. Rev.*, **135**, 4202–4213.

Steiger, S. M., and Coauthors, 2013: Circulations, bounded weak echo regions, and horizontal vortices observed within long-lake-axis-parallel–lake-effect storms by the Doppler on Wheels. *Mon. Wea. Rev.*, **141**, 2821–2840.

Weckwerth, T. M., and Coauthors, 2004: An overview of the International H2O Project (IHOP_2002) and some preliminary highlights. *Bull. Amer. Meteor. Soc.*, **85**, 253–277.

8. FIGURES

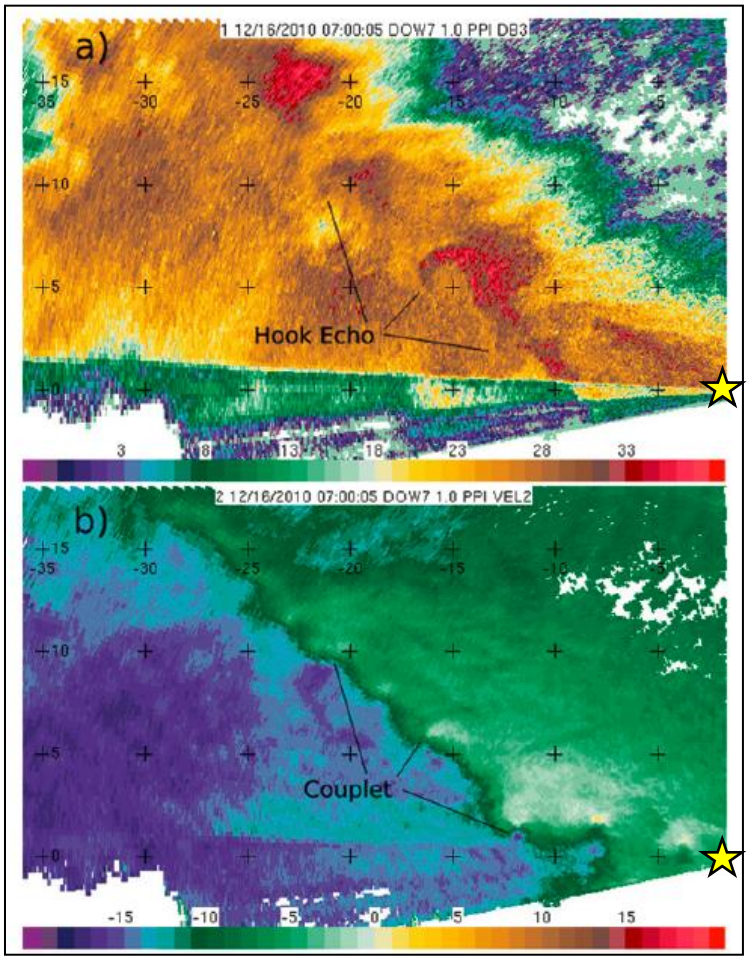

Figure 1. DOW7 observations of a) radar reflectivity (dBZ) and b) Doppler radial velocity (m s^{-1}) at 07:00:05 UTC 16 December 2010. Note how the hook echoes in the reflectivity field correspond to the couplets in the velocity field. The yellow star denotes the location of DOW7 (Figure courtesy: Steiger et al., 2013).

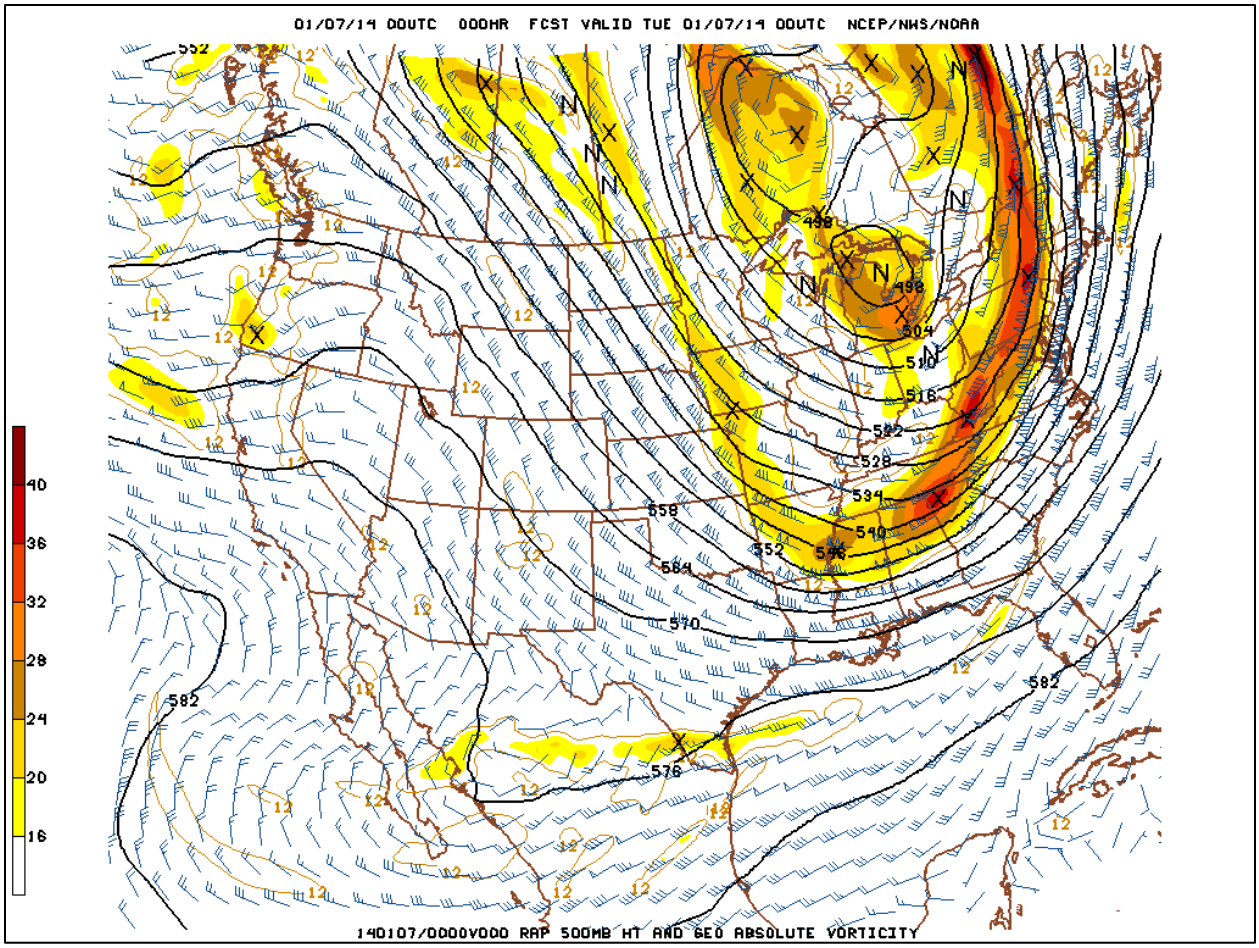

Figure 2. Rapid Refresh (RAP) model 500-hPa analysis valid at 0000 UTC 7 January 2014. Geopotential height (Dm) is in solid black contours, winds barbs (kts) are in blue, and geostrophic absolute vorticity is shaded every 4 x 10^{-5} s^{-1} starting at 16 x 10^{-5} s^{-1} (Figure courtesy: OWLeS Field Catalog - http://catalog.eol.ucar.edu/owles).

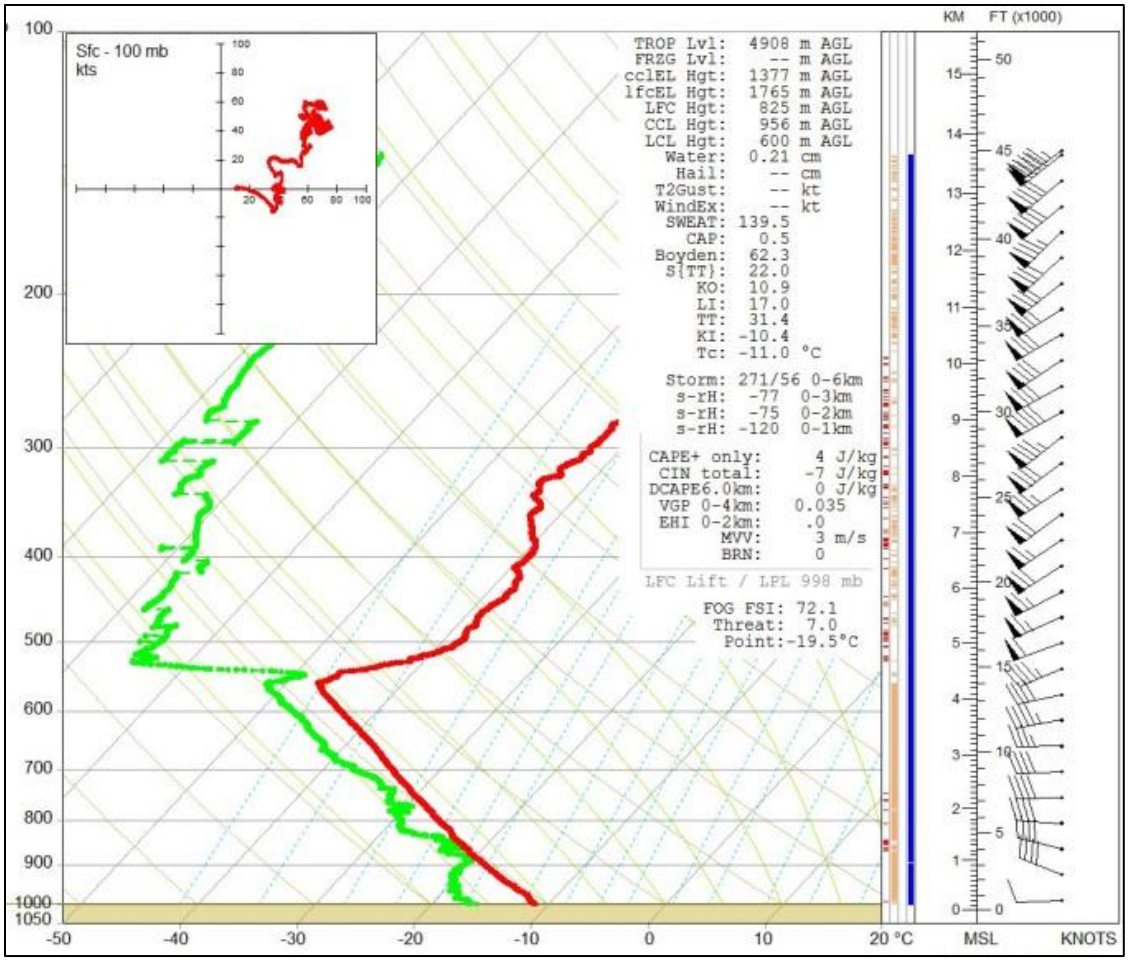

Figure 3. Sounding launched at 0816 UTC 7 January 2014 from Henderson Harbor, NY (denoted by the red star in Fig. 4). The red line indicates temperature (˚C) and the green line indicates dewpoint temperature (˚C). Winds (kts) are plotted along the right side of the image using standard meteorological notation.

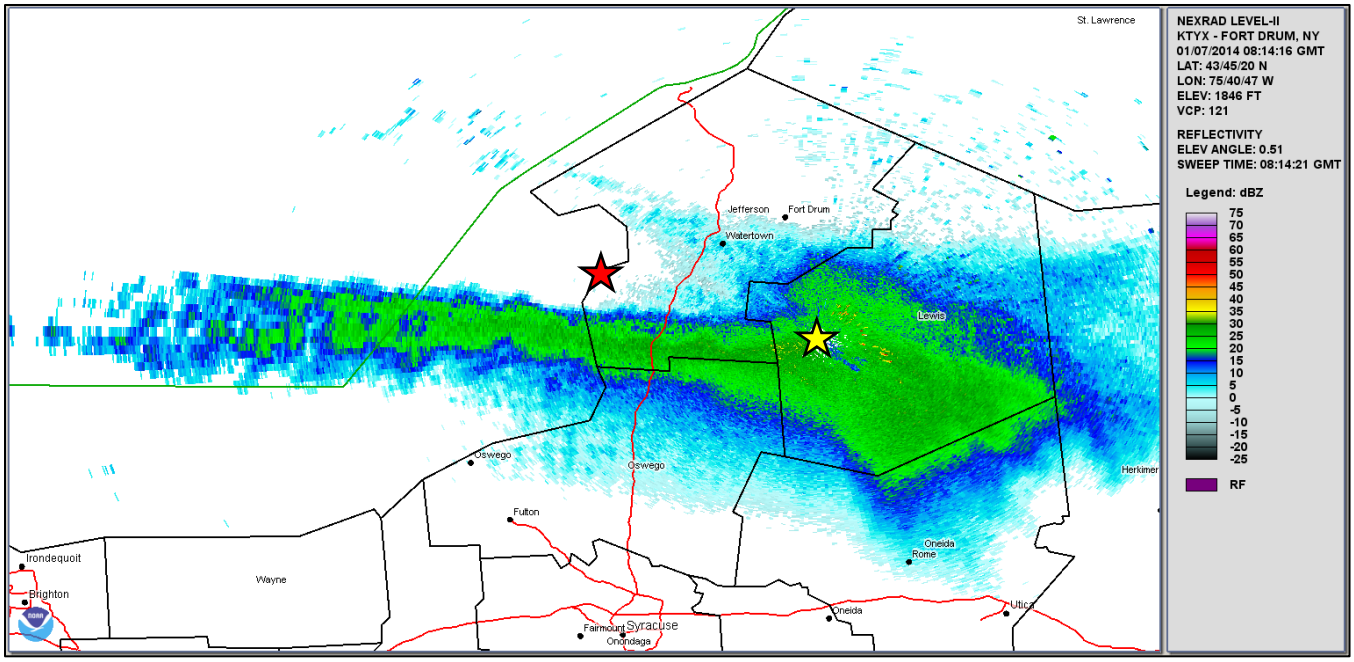

Figure 4. Radar reflectivity at 0.5˚ from Montague, NY (KTYX), at 08:14:16 UTC 7 January 2014. The red star indicates the location of the sounding launched at 0816 UTC at Henderson Harbor, NY (see Fig. 3). The yellow star indicates the location of KTYX (Figure created using the NOAA Weather and Climate Toolkit).

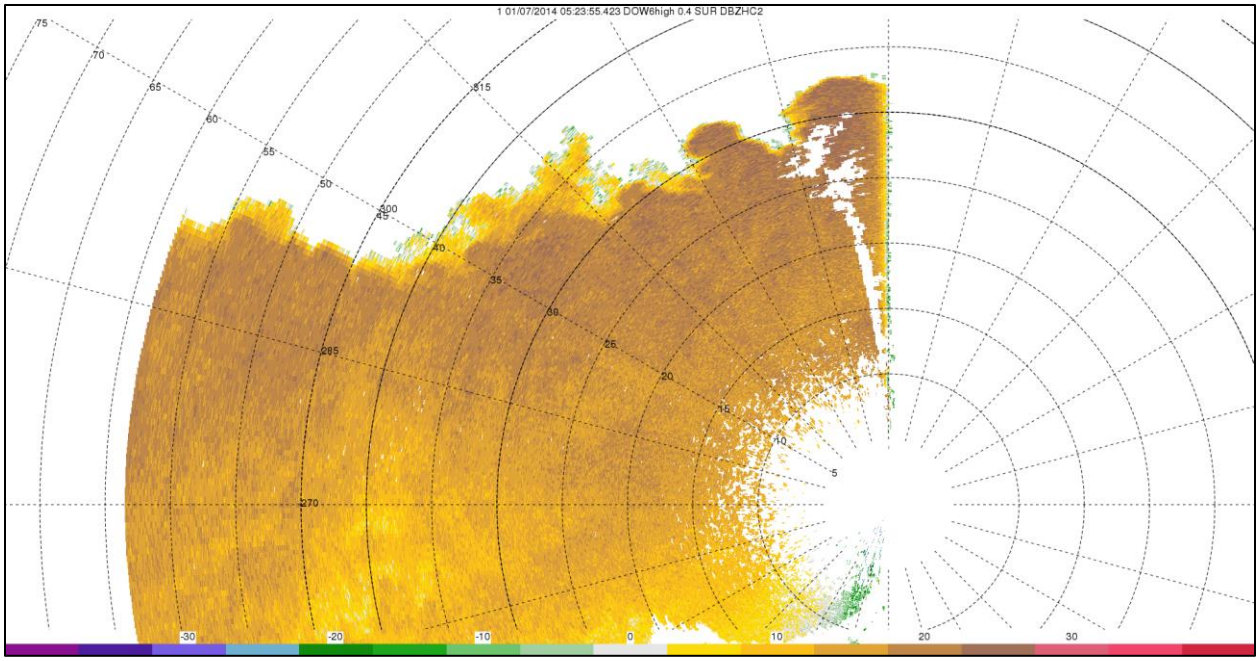

Figure 5a. 0.4˚ DOW6 reflectivity (dBZ) at 05:23:55 UTC 7 January 2014. Range rings are plotted every 5 km and azimuth angles are plotted every 15˚.

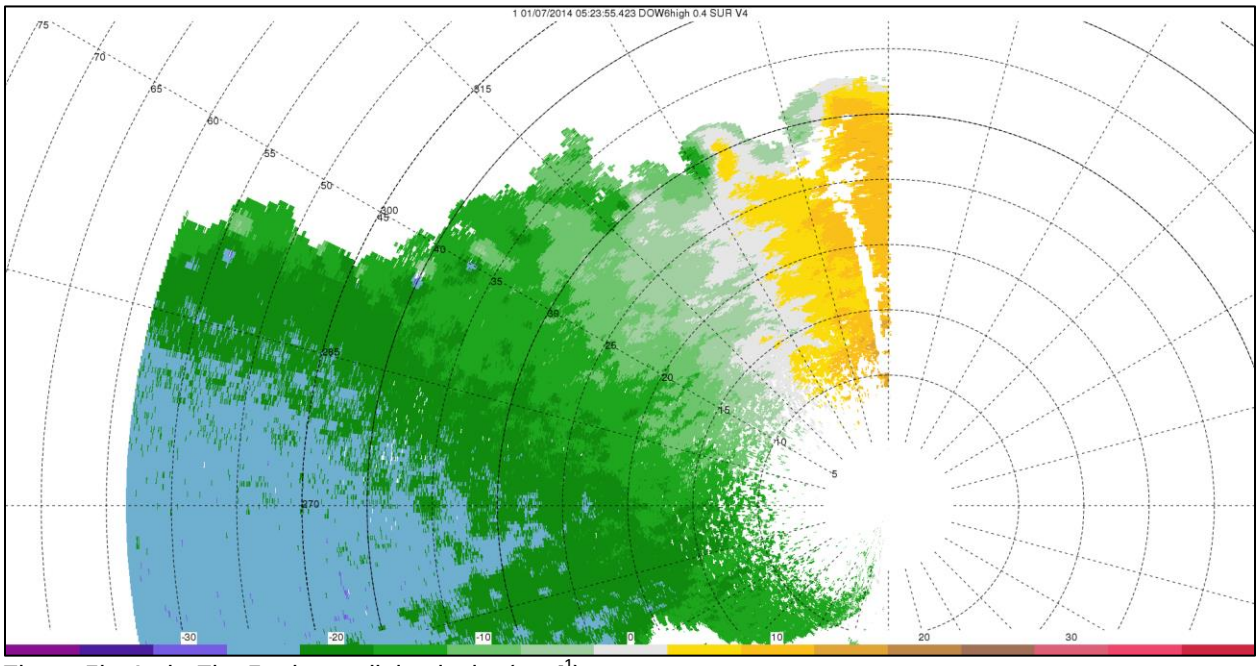

Figure 5b. As in Fig. 5a, but radial velocity (m s^{-1}).

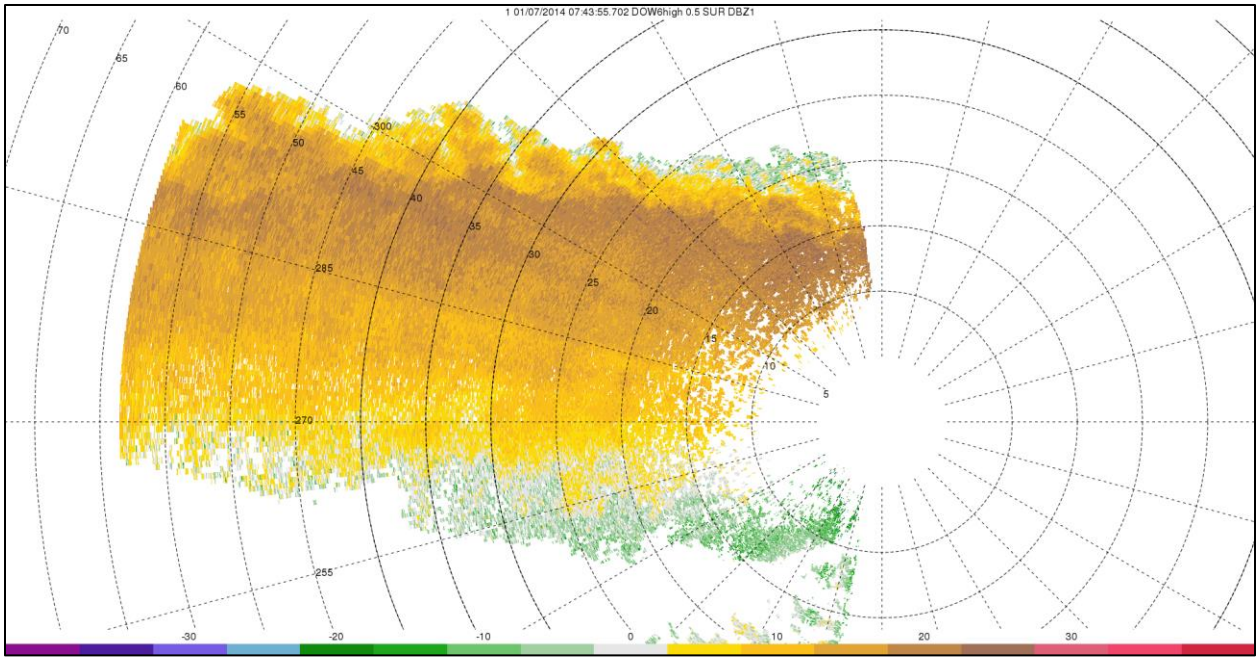

Figure 6a. As in Fig. 5a, but at 07:43:55 UTC.

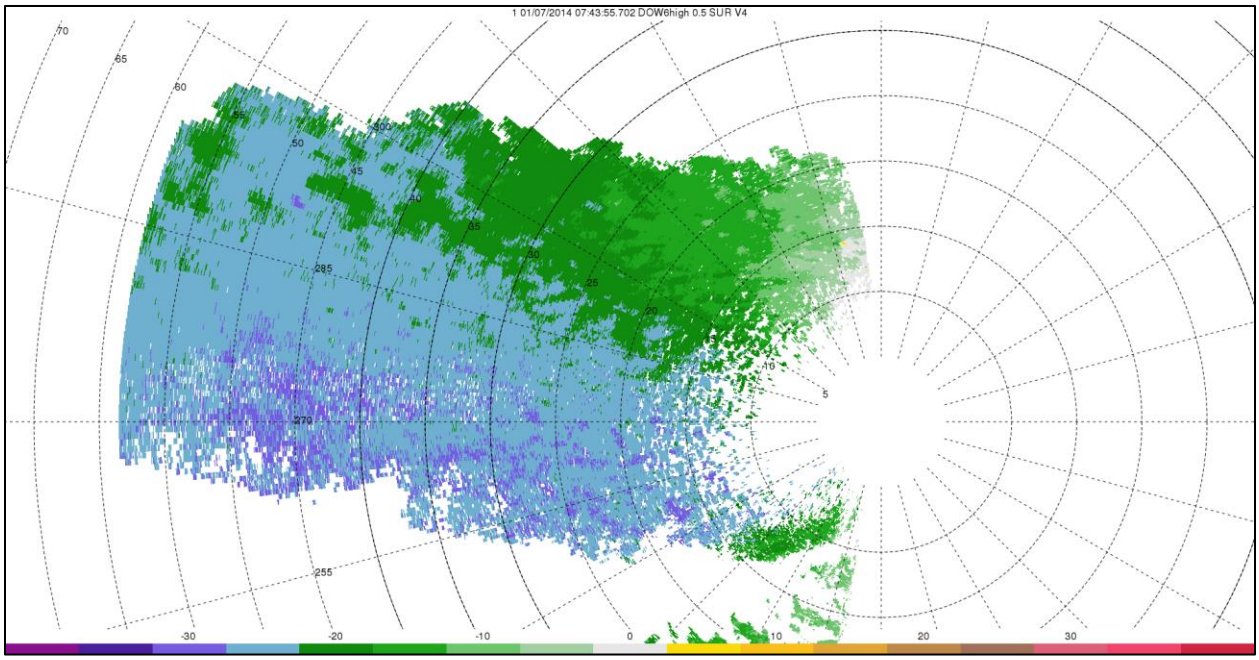

Figure 6b. As in Fig. 5b, but at 07:43:55 UTC.

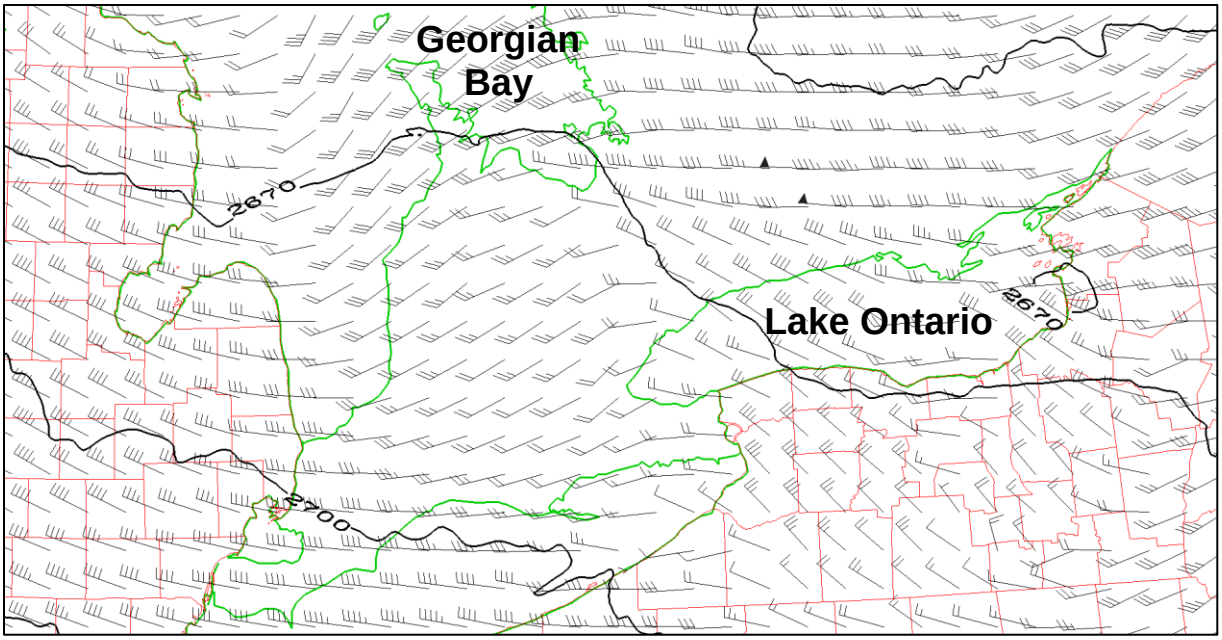

Figure 7. 700-hPa analysis valid at 0700 UTC from a 0300 UTC/7 January 2014 RAP-initialized Weather Research and Forecasting simulation. Geopotential height (m) is in solid black contours and winds barbs (kts) are in black using standard meteorological notation.

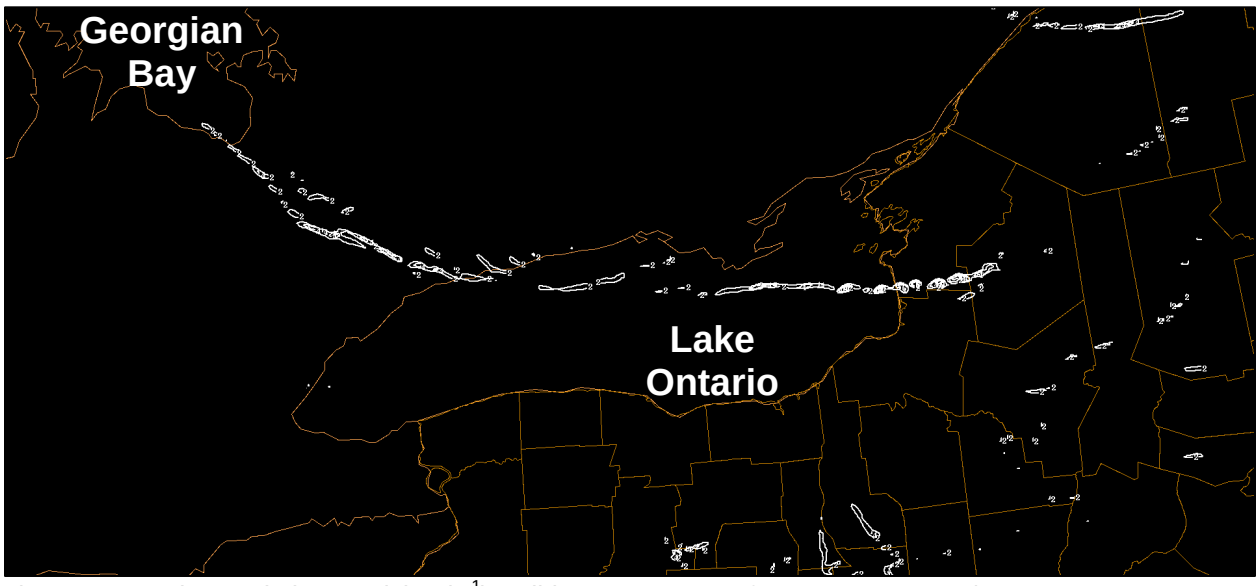

Figure 8. 900-hPa relative vorticity (s^{-1}) valid at 0700 UTC from a 0300 UTC/7 January 2014 RAP-initialized Weather Research and Forecasting simulation.

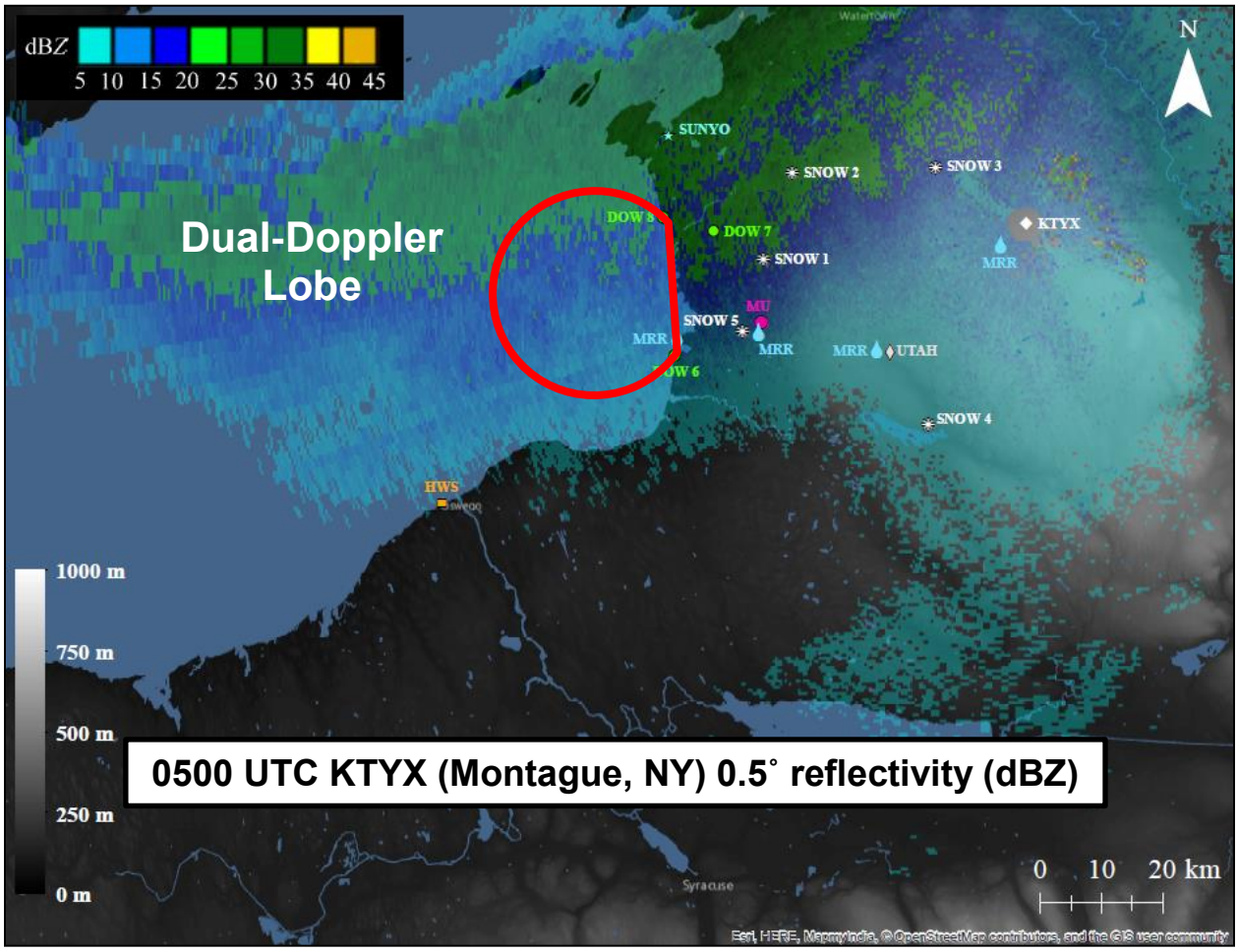

Figure 9. OWLeS asset map from 7 January 2014. The approximate dual-Doppler lobe from DOW6 and DOW8 is drawn in red. The three DOW locations are labeled and marked with green dots, the Montague, NY (KTYX), radar location is labeled and marked with a white diamond, mobile snow-sampling teams are labeled and marked with white asterisks, Microwave Rain Radars (MRR) are labeled and marked with blue rain drops, and the sounding locations are labeled and marked with a variety of colors/symbols (HWS, SUNYO, UTAH, and MU; Figure courtesy: Christopher Johnston, University of Illinois at Urbana-Champaign).

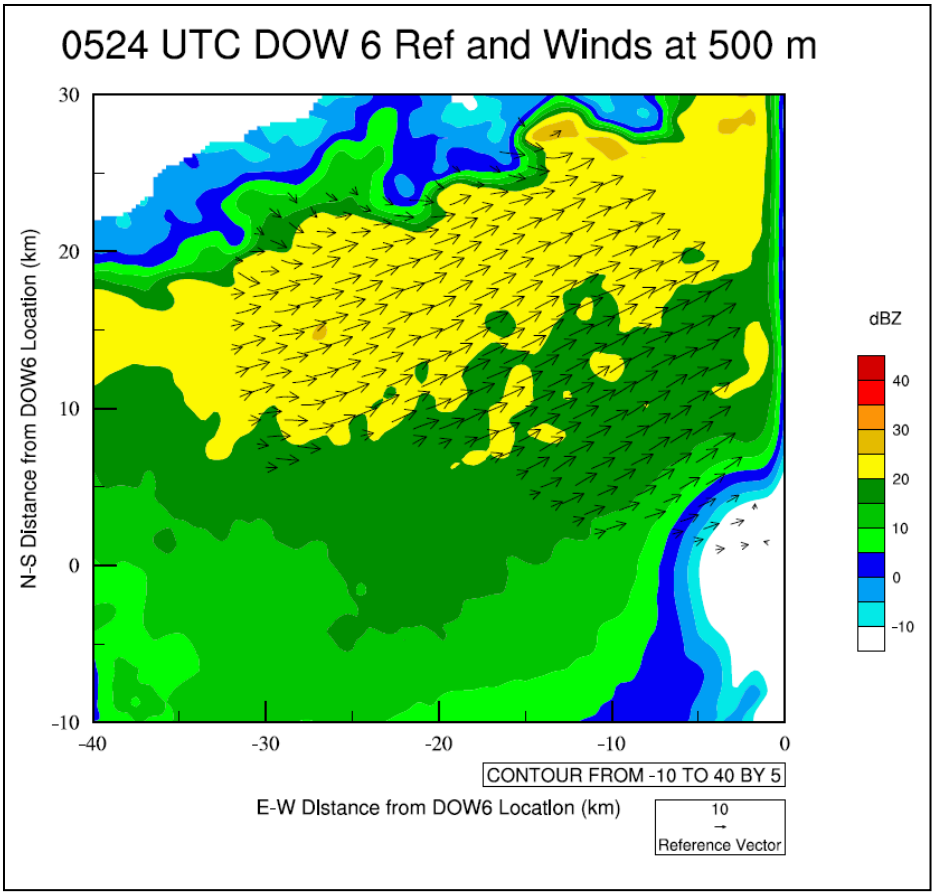

Figure 10. Dual-Doppler wind synthesis at 500 m AGL at 0524 UTC 7 January 2014. Reflectivity from DOW6 is plotted every 5 dBZ starting at -10 dBZ and is overlaid with DD-derived winds (black vectors).

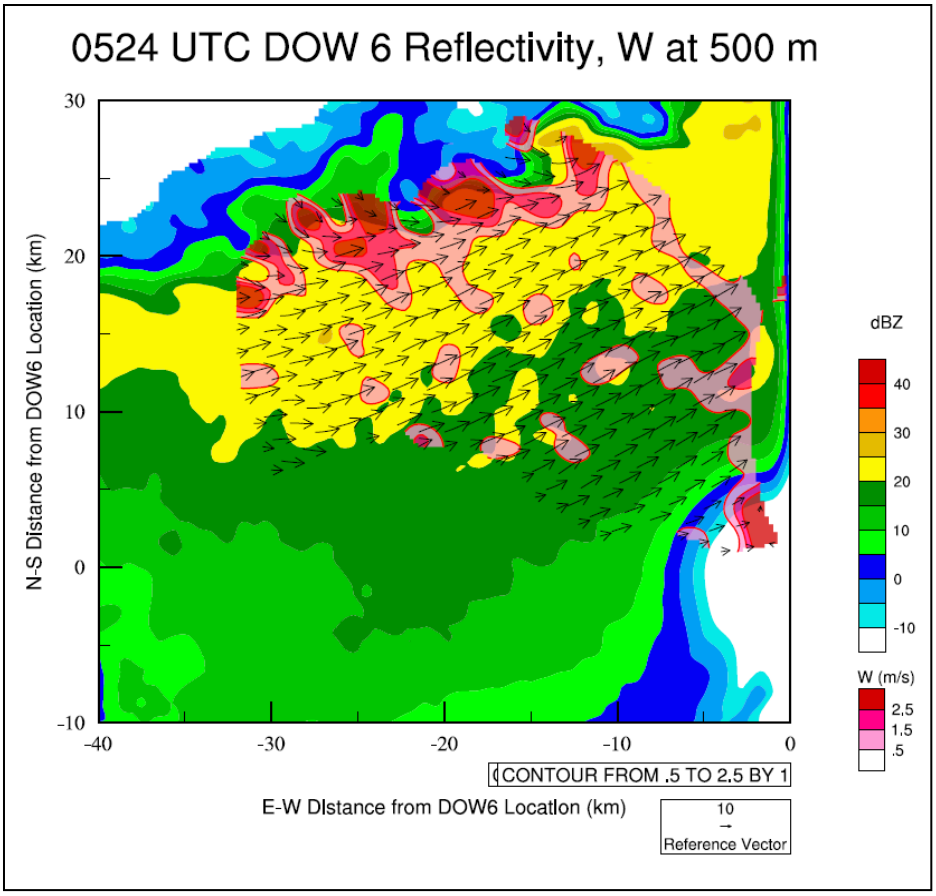

Figure 11. As in Fig. 10 overlaid with DD-derived vertical velocity (red fill colors, only positive values shown) plotted every 1 m s^{-1} starting at 0.5 m s^{-1}.

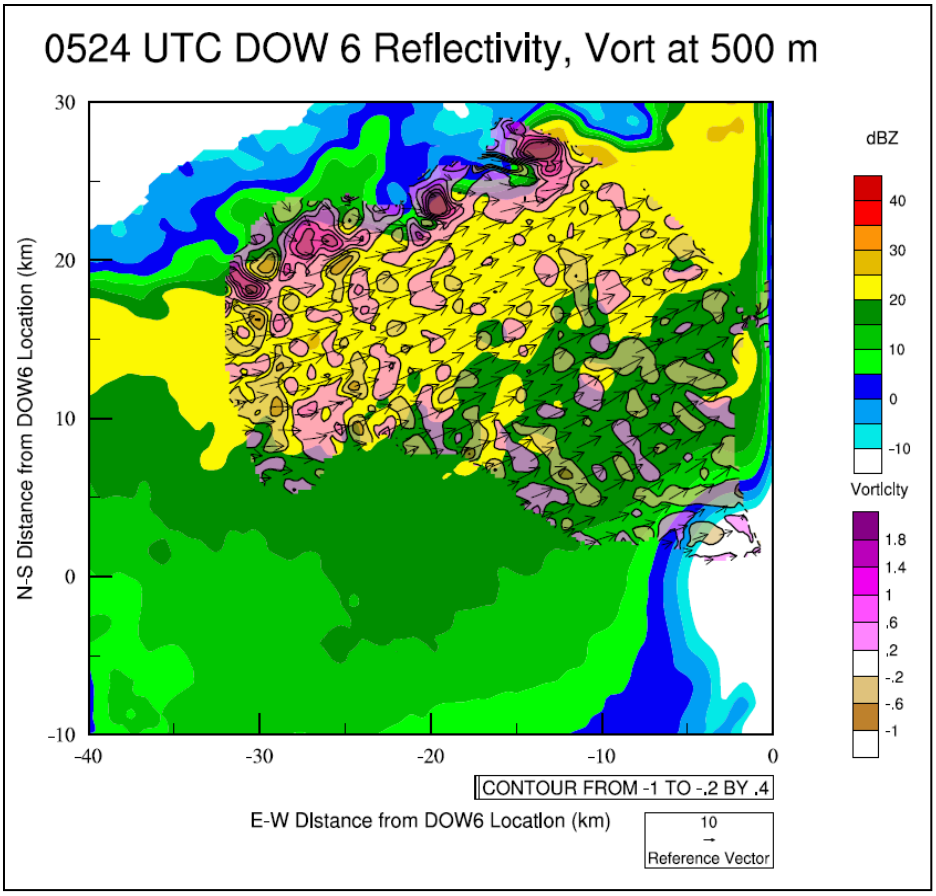

Figure 12. As in Fig. 10 overlaid with DD-derived relative vertical vorticity (pink and brown fill colors) plotted every 0.4 x 10^{-2} s^{-1}.

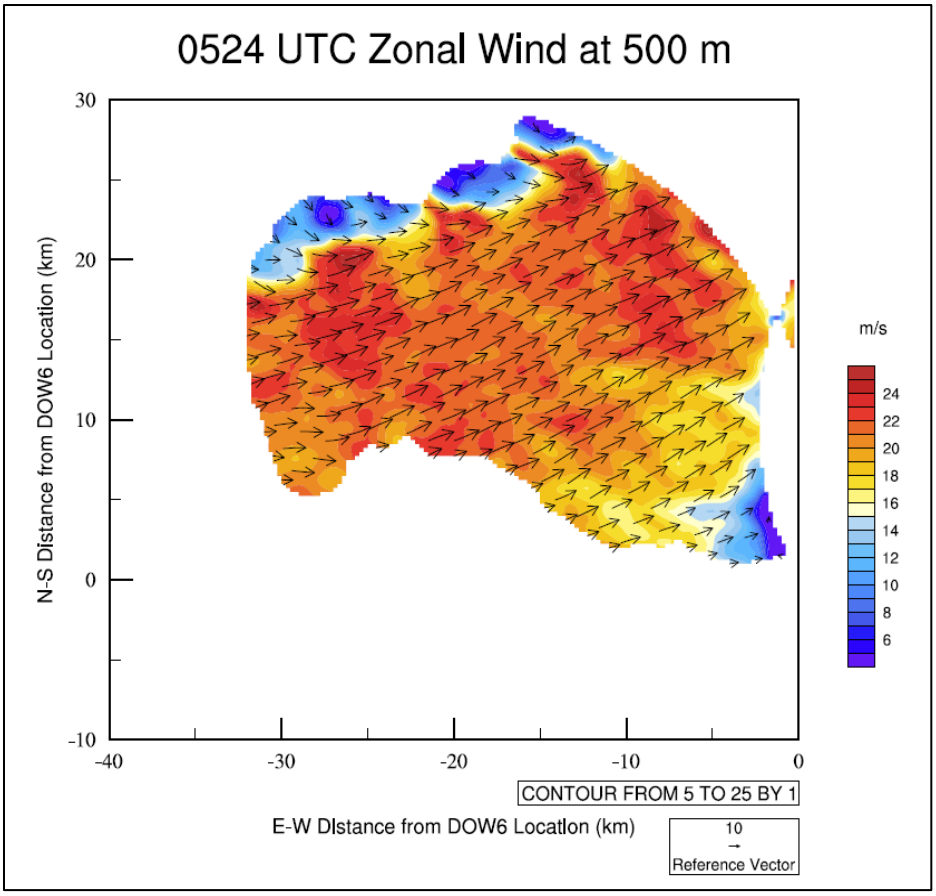

Figure 13. Dual-Doppler wind synthesis at 500 m AGL at 0524 UTC 7 January 2014. DD-derived winds (black vectors) are plotted along with the zonal wind component (shaded) every 2 m s^{-1}.

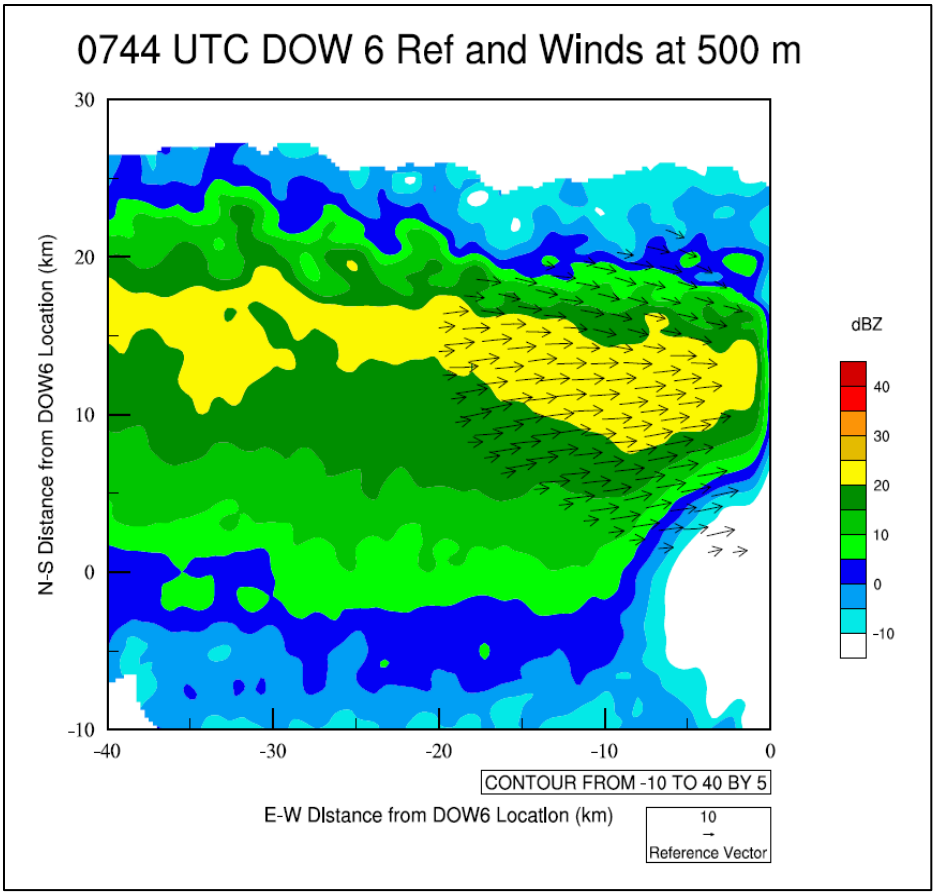

Figure 14. As in Fig. 10, but at 0744 UTC.

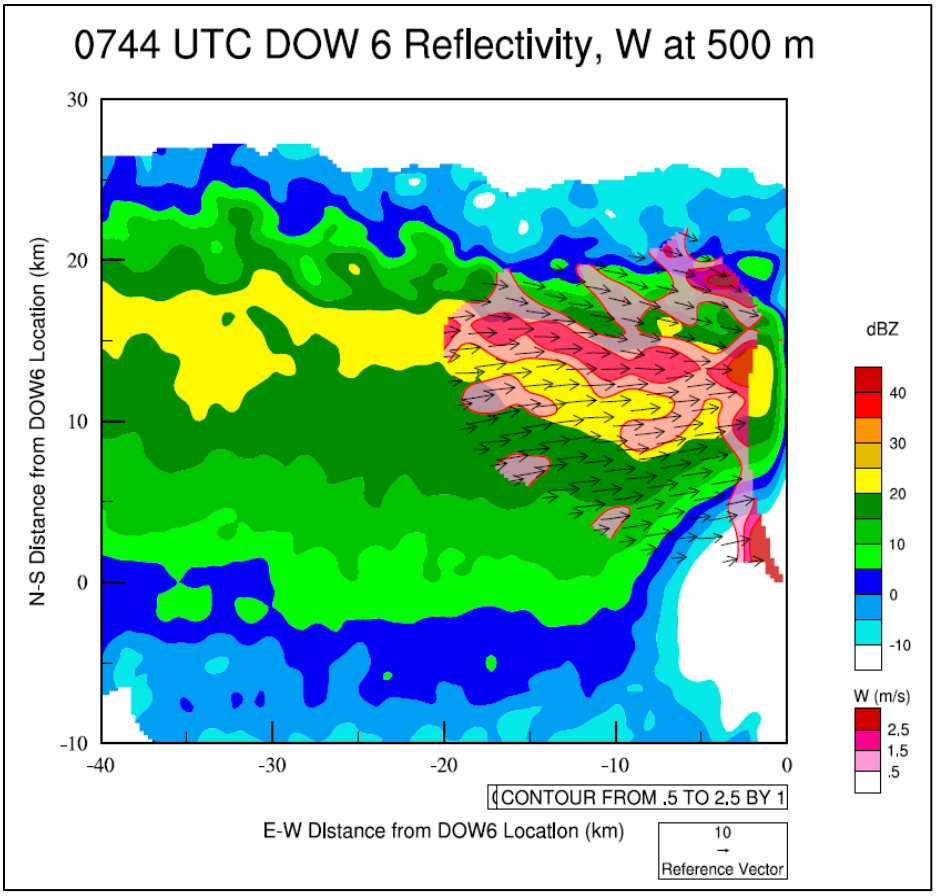

Figure 15. As in Fig. 11, but at 0744 UTC.

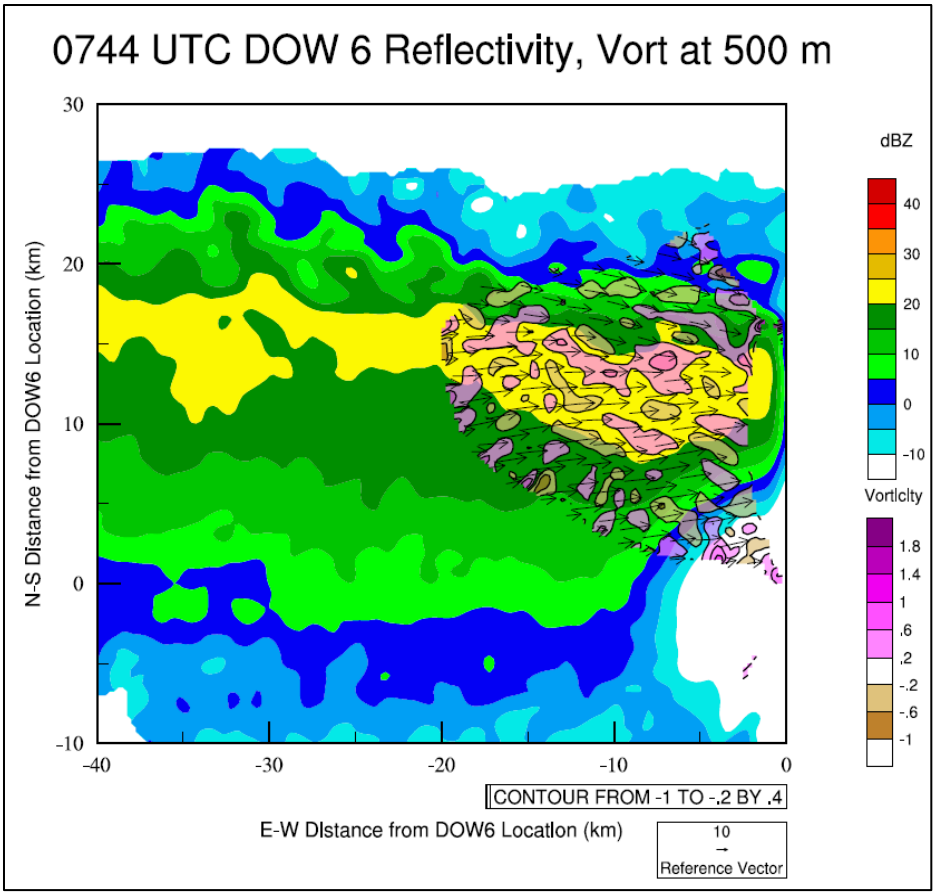

Figure 16. As in Fig. 12, but at 0744 UTC.

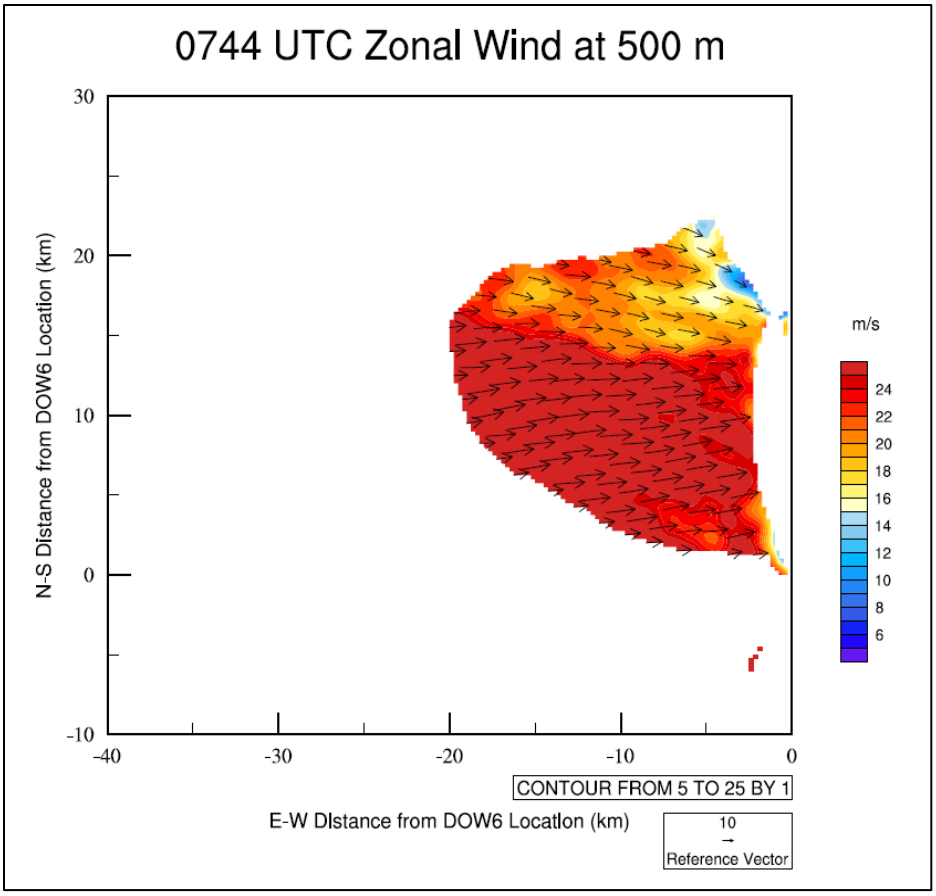

Figure 17. As in Fig. 13, but at 0744 UTC.